

The Development of a Novel Large Area Building Integrated Solar Collector for Pool Heating

Authors: T.N. Anderson¹, M. Duke², J.K. Carson², R. Kunne Meyer² and B. Smith³

¹School of Engineering, Deakin University,
Pigdons Rd, Geelong Vic 3217

²Department of Engineering, University of Waikato,
Hamilton NZ 3240

³WaikatoLink Ltd, University of Waikato,
Hamilton NZ 3240

timothy.anderson@deakin.edu.au

ABSTRACT

Unglazed solar collectors have often been used as a means of providing low cost heating to swimming pools. However, these systems are typically polymer style “mats” that are laid on top of a roof, often leading to poor aesthetics due to their lack of integration with the building itself.

This study charts the development of a novel large area unglazed building integrated solar pool heating system (BIT), based on long run sheet metal roofing, from its initial conceptualisation through to its implementation. It discusses the design of the building integrated solar collector modules, the assessment of their performance through theoretical modelling and experimental validation. Subsequently, it shows the scaling of laboratory scale testing to a large area array through modelling and discusses the performance of the system in the “as-built” configuration.

In doing this, it provides a succinct illustration of the design process for the development of the University of Waikato’s building integrated pool heating system.

Keywords – building integrated solar collector, pool heater, product development

INTRODUCTION

The integration of solar hot water systems into roofs has three potential advantages over conventional ‘bolt on’ systems; installation of both the roof and solar panel occur at the same time, reduced material cost and superior aesthetics.

Integration is however not straightforward making it difficult to turn the potential into a reality. One of the major barriers to the uptake of integrated systems is the mismatch between the technology and installation methods of the roofing industry and the solar industry. In New Zealand and Australia, roof product manufacturers are generally conservative with long lead times for product development. In comparison the solar industry is experiencing a period of rapid growth and innovation.

The use of water cooled solar collectors as building elements has, until recently, been largely ignored. Ji et al. (2006) and Chow et al. (2007) both examined a photovoltaic/thermal (PVT) system for integration into building walls in Hong Kong. They showed that these systems could make useful heat gains while also acting to reduce thermal load on the building. However, these systems were essentially PVT

panels integrated *onto* a building rather than *into* the building (i.e. individual PVT collectors are used as the material for the wall, rather than using the wall as the material for a PVT collector).

Similarly, Kang et al. (2006) discussed the performance of a roof integrated solar collector which again consisted of a series of “standalone” collectors used as a roof. Again, this system although integrated *onto* the building is not integrated *into* the building. In a study by Probst and Roecker (2007) this method of integrating solar collectors was considered to be “acceptable” to architects. However they note that in the future, building integrated solar collectors “should be conceived as part of a construction system”.

Although somewhat self-evident the comments of Probst and Roecker appear to have been overlooked by the research community. Medved et al. (2003) however examined an unglazed solar thermal system that could be truly integrated into a building. In their system they utilised a standard metal roofing system as a solar collector for water heating. They found that in a swimming pool heating system, that they were able to achieve payback periods of less than 2 years. This translated to a reduction of 75% in the time taken to pay for a glazed solar collector system. Similar systems to that of Medved et al. have been developed and discussed by Bartelsen et al. (1999) and Colon and Merrigan (2001).

In New Zealand and Australia long run metal roofing is widely used for domestic, commercial and industrial applications. A typical example of such a roof is shown in Fig. 1.



Fig. 1 Long Run Metal Roof

Long run roofing comprises a substrate of steel strip, commonly 0.40 mm or 0.55 mm thick and coated with a 45% zinc-55% aluminium alloy. A corrosion inhibitive primer and top coat (paint) are applied to the outer surface and is available in a wide variety of colours. The finished sheet is then roll formed or folded into the desired profile. Moreover, their low cost, high durability, aesthetics and relatively good thermal conductivity make the material well suited to use as solar collector.

BUILDING INTEGRATED SOLAR WATER HEATER (BIT) – THE CONCEPT

The system developed in this study is unique in a number of ways. Unlike many of the systems that have been proposed, this system is designed to be directly integrated into the roof of a building, in this case a troughed sheet metal roof. As has been discussed, long run standing seam and troughed sheet roofs are typically made from coated steel, although copper or stainless steel could be used. Typically they are rolled into a shape that gives the roof product stiffness and strength and when assembled as a roof they are weather proof.

During the manufacturing process in addition to the normal troughed shape, channels are added to the trough for the thermal cooling medium to travel through (Fig. 2). An absorber sheet, analogous to the fin of a finned tube absorber, is bonded into the trough. The channels formed in the trough are enclosed by this sheet; thus forming a riser tube having an inlet and outlet at opposite ends of the trough to which heat can be transferred. Fluid is pumped through a manifold (header tube), through these “riser” tubes and out through a manifold (header tube) before being fed to a heat exchanger that removes the heat from the fluid.

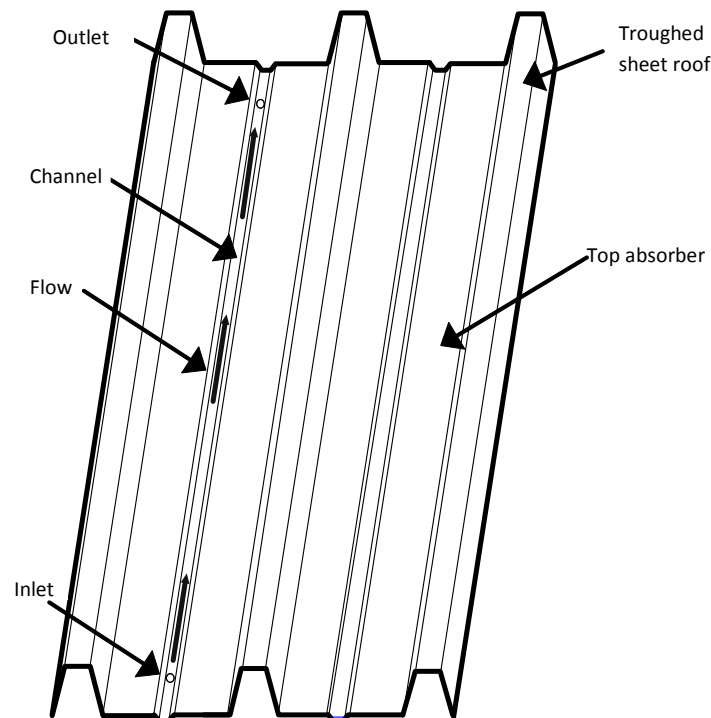


Fig. 2 Building integrated solar collector

The unique design of the collector and some of the design goals presented a number of challenges. This was mainly due to the fact that the material was galvanised and dip coated in black paint, so could not be easily welded without removing both coatings. To overcome this, the roof profile was folded using a CNC folder and holes were drilled to allow fluid into the underside of the coolant channel. Nipples were silver soldered to the rear surface to allow a manifold to be attached. The top absorber sheets were glued to the roof section, and the channels sealed, with a high temperature silicone adhesive sealant thereby forming a standalone watertight collector with a roof profile, as shown in Fig. 3.



Fig. 3 Prototype building integrated solar collector

THEORETICAL EFFICIENCY OF THE COLLECTOR

To determine the theoretical performance of the building integrated solar collector a validated one-dimensional steady state thermal model for an unglazed solar collector was utilised (Anderson *et al.*, 2009).

Under these conditions the useful heat gain can be calculated using Equation 1.

$$Q = AF_R [(\tau\alpha).G'' - U_L(T_{in} - T_a)] \quad (1)$$

Where the useful heat gain (Q) can be represented as a function of the collector area (A), the heat removal efficiency factor (F_R), the transmittance-absorptance product of the collector ($\tau\alpha$), the solar radiation (G''), the collector heat loss coefficient (U_L) and the temperature difference between the collector inlet temperature (T_{in}) and the ambient temperature (T_a).

Of these parameters, the transmittance-absorptance product is the only one that is based solely on a physical property of the collector material. The absorptance provides a measure of the proportion of the incoming solar radiation captured by the absorber surface, in this case the black steel. The transmittance component measures the portion of the radiation transmitted by any glazing layer and in this case for an unglazed collector it was assumed to be equal to unity. Therefore, to understand the optical characteristics of the building integrated collector it was decided to determine its absorptance characteristics over the Air Mass 1.5 solar spectrum.

To determine the absorption of the colour coated mild steel, the diffuse reflectance (ρ) of a black sample was measured at 20nm wavelength intervals between 300nm to 2500nm using a spectrophotometer and a 6° integrating sphere at Industrial Research Limited (Wellington, NZ). Based on the reflectance measurement results shown in Fig. 4, it was possible to determine the absorptance (α) component using Equation 2, as it

was assumed that coloured steel is an opaque surface with zero transmittance (Duffie and Beckman, 2006).

$$\alpha = 1 - \rho \quad (2)$$

By integrating the absorptance derived from the measurements of the reflectance over the range of AM1.5 wavelengths it was found that the black painted steel had relatively constant reflectance characteristics with an absorptance value of 0.95.

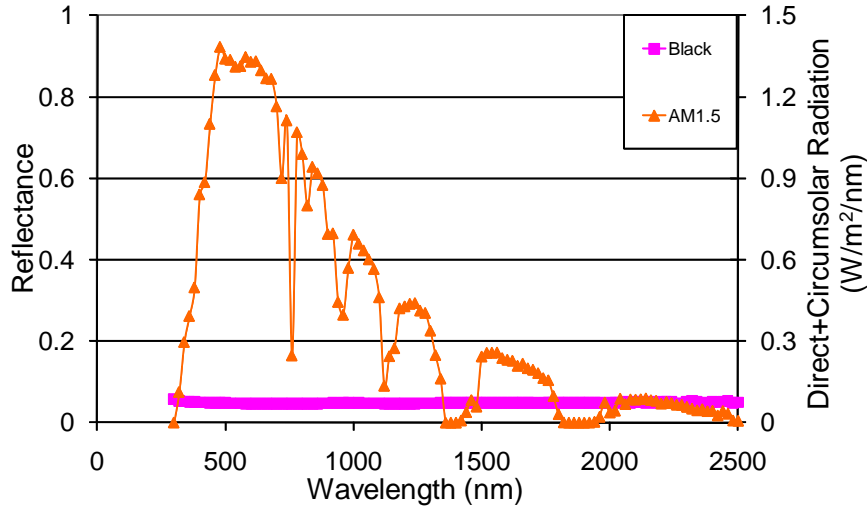


Fig. 4 Reflectance from black steel sample over AM1.5 spectrum

The heat removal efficiency factor (F_R) can be derived from Equation 2, which accounts for the mass flow rate in the collector (\dot{m}) and the specific heat of the collector fluid (C_p).

$$F_R = \frac{\dot{m}C_p}{AU_L} \left[1 - e^{-\frac{AU_{loss}F'}{mC_p}} \right] \quad (2)$$

To determine the heat removal efficiency factor it is necessary to calculate a value for the corrected fin efficiency (F'). This is done by first calculating the fin efficiency (F) using Equation 3. This determines the efficiency of the finned area between adjacent tubes and takes into account the influence of the tube pitch (W) and the tube width (d). Furthermore, the coefficient (M) accounts for the thermal conductivity of the absorber and is derived from Equation 4.

$$F = \frac{\tanh\left(M \frac{W-d}{2}\right)}{\left(M \frac{W-d}{2}\right)} \quad (3)$$

$$M = \sqrt{\frac{U_L}{K_{abs}L_{abs}}} \quad (4)$$

Therefore, the corrected fin efficiency (F') can be calculated using Equation 5, noting that there is not bond resistance term as would be found in the analysis of a finned tube analysis and where the overall heat loss coefficient (U_L) of the collector is the summation of the collector's edge (negligible for a large array), bottom and top losses.

$$F' = \frac{\frac{1}{U_L}}{W \left[\frac{1}{U_L(d + (W - d)F)} \right] + \frac{1}{\pi d h_{fluid}}} \quad (5)$$

For unglazed collectors as used in this study, the top loss coefficient is a function of both radiation and wind. As such it is necessary to calculate the top loss coefficient (U_{top}) by taking the summation of the individual contributions of radiation, natural and forced convection. Under such conditions, the heat loss due to radiation can be expressed as a radiation heat transfer coefficient in terms of the sky temperature (T_s), the mean collector plate temperature (T_{pm}) and the plate emissivity (ε_p) as shown in Equation 7.

$$h_r = \sigma \varepsilon_p (T_{pm}^2 + T_s^2)(T_{pm} + T_s) \quad (7)$$

where the sky temperature is represented by the modified Swinbank equation as a function of the ambient temperature as shown in Equation 8 (Fuentes, 1987).

$$T_s = 0.037536T_a^{1.5} + 0.32T_a \quad (8)$$

Furthermore, the losses due to natural and forced convection must also be taken into account. The forced convection heat transfer coefficient (h_w) can be calculated using a correlation in terms of wind velocity (v), as shown in Equation 9 (Watmuff et al, 1977), while the natural convection loss (h_{nat}) can be represented by a function of the temperature difference between the mean collector plate temperature (T_{pm}) and the ambient temperature (T_a) as shown in Equation 10 (Eicker, 2003).

$$h_w = 2.8 + 3.0v \quad (9)$$

$$h_{nat} = 1.78(T_{pm} - T_a)^{1/3} \quad (10)$$

Using this method it is possible to determine an overall convection heat transfer coefficient (h_c) by combining both forced and natural convection heat transfer as shown in Equation 11. Subsequently by taking the summation of the convection and radiation losses, it is possible to determine the overall top loss heat transfer coefficient (U_{top}) for the unglazed collector. Similarly, for an unglazed collector installed in an array with no back insulation, it can be assumed that radiation losses between the back surface and the ground are minimal due to the low emissivity coating on the colour steel roof and also the small temperature differences between the surfaces. However, both natural convection and wind losses are still present and as such the back loss was also taken to be represented by Equation 11 (Eicker, 2003).

$$h_c = \sqrt[3]{h_w^3 + h_{nat}^3} \quad (11)$$

It is then possible to calculate the useful heat gain from the solar collector. By taking the ratio of the useful heat gain to the total radiation falling on the collector area (Q/AG) we can subsequently determine the theoretical efficiency of the collector as shown in Figure 5.

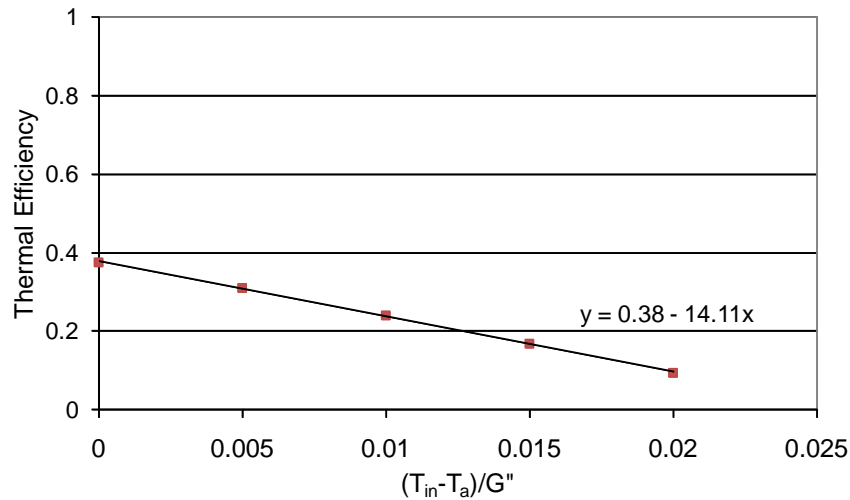


Fig. 5 Theoretical efficiency of unglazed black collector

MODELLING THE COLLECTOR CONTRIBUTION TO POOL HEATING

Having determined the theoretical performance of the unglazed black BIT collector it was decided to implement these parameters into the Canadian Renewable Energy Network's (2010) Enerpool Pro package, to determine the potential output from a large BIT array heating the University of Waikato outdoor diving pool (~400m³ with 100m² surface area).

For the simulations, it was assumed that the pool would operate on the "swimmable days" concept between December and March under typical meteorological year (TMY) conditions for Hamilton (Anderson et al, 2007). Furthermore it was assumed that the array would have an area of approximately 100m², made up of two banks of collectors, with fourteen rows of four collectors in series. The daily makeup water loss was assumed to be 1000L and no pool cover would be used.

Now to determine the effect of the collector on the pool temperature, two simulations were undertaken: in the first, the pool was modelled without the collector being active, in the second, the collector was allowed to contribute to the heating of the pool. From these two simulations it was found that the collector could potentially increase the pool temperature by over 2°C during the pools operational months, as shown in Table 1.

Table 1: Average monthly pool temperatures with and without heating for a TMY

Month	Average Pool Temperature (°C) without heating	Average Pool Temperature (°C) with heating
December	21.7	24.8
January	22.2	25.3
February	21.9	24.6
March	21.7	24.1

On this basis, it can be seen that there is a distinct benefit to having a solar heating system operating on the diving pool, as a means to improve swimmers comfort.

EXPERIMENTAL PERFORMANCE OF POOL HEATING SYSTEM

Having demonstrated the potential benefits of having a solar heating system on the diving pool a decision was made to construct a heating system using the BIT panels for initial operation during the summer of 2009/10. In this regard a special frame was made so that the BIT panels for heating the dive pool also acted as a sun shade (Fig. 6).

The roof was made up of 120 panels in six rows, with the panels not uniformly distributed amongst these rows due to the shape of the roof. Once the water was heated in the collector, it was fed into a heat exchanger. This water was cooled by the water from the pool, which in turn was heated, and returned to the pool. Flow meters were used to measure the flow rate of water through the collectors. Thermocouples were used to measure temperatures at various locations in the system, and the solar radiation was measured using a pyranometer (Fig. 7).

It can be seen that the BIT system looks like a conventional long run painted steel roof. The outer parts of the roof were made from standard roofing and integrated seamlessly with the BIT. This shows that it is possible to use long run roofing material not only for BIT but in conjunction with it. It should also be noted that the entire roof (without the plumbing) was installed by roofers with some training of how to handle the BIT panels.

During initial testing, there were major problems with flow variation in the BIT panels. Large areas had little or no flow leading to hot spots and low overall system efficiency. This problem was somewhat resolved through modifications to the plumbing layout, but not completely.



Fig. 6 Unglazed BIT Dive Pool System

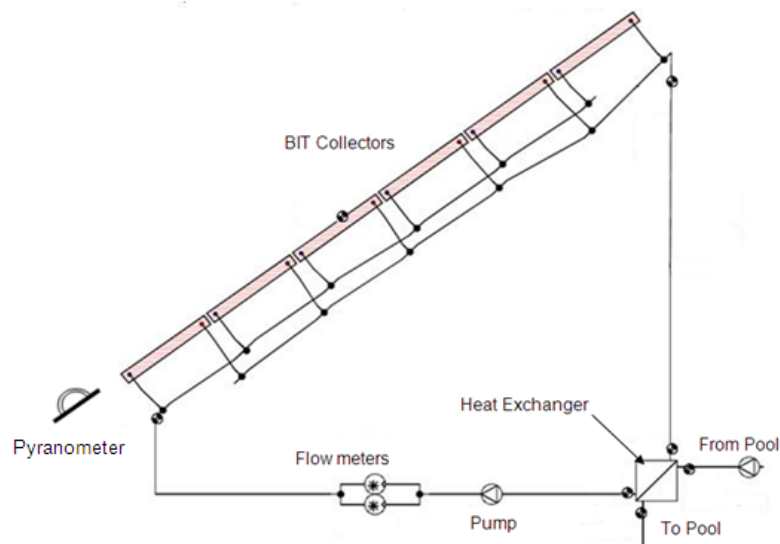


Fig. 7 Schematic of Dive Pool System

Now in order to illustrate the potential effect of the BIT heating system, temperatures of both the dive pool and the adjacent main pool were monitored by staff as part of routine maintenance procedures over the 2008/09, before the heating system was operational, and during 2009/10 season, while the collector was operational. These were manually collected normally three times a day using a digital thermometer, typically between 12 pm – 6 pm. Although temperatures were not recorded every day, the data collected still gives a very good indication of the performance of the BIT system.

Now in Fig. 8 it can be seen that during the summer of 2008/09 with no BIT heating system, the temperatures of the two pools are very close over the entire season. However during the summer season of 2009/10 with the aid of the BIT system (Fig. 9), the average difference between the dive pool and main pool temperatures increased noticeably. From the data, it was found that without the BIT heating system the dive pool was on average 0.2 °C warmer than the main pool however the addition of the heating system increased this by more than a degree, to 1.3°C (Fig. 10). Although this does not sound a great difference a straw poll of both staff and swimmers found they

believed the dive pool to be noticeably warmer. In addition it should be noted that compared to the 2008/09 season, the 2009/10 main pool temperature is 0.8°C lower, showing the 2008/09 summer was sunnier and warmer than the 2009/10 summer.

Based on the data collected over the summer of 2009/10 the average efficiency of the BIT system over the season was found to be 22.4%. This compares well with the predicted efficiency for a TMY from the simulation, which suggested an efficiency of 26%. The reasons for the difference however include minor differences between the modelled and installed system, uneven flow distribution and lower fin efficiency than theoretically modelled due to manufacturing discrepancies. However further investigations are being undertaken to understand and optimise the system.

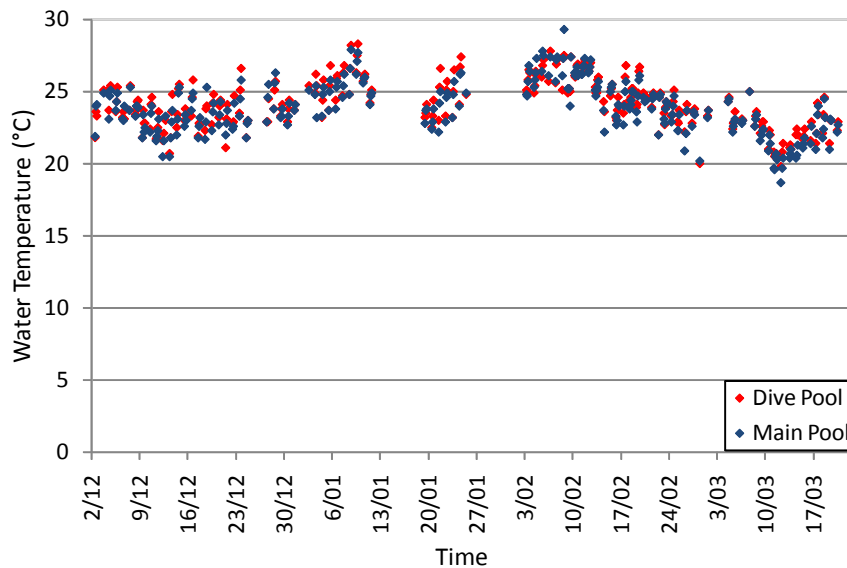


Fig. 8 Pool temperatures for summer 2008/09 (no heating)

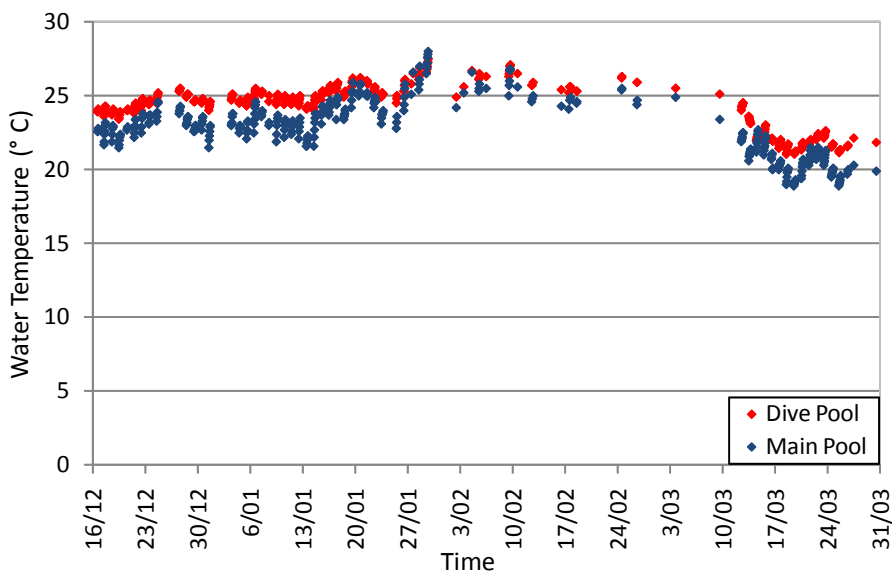


Fig. 9 Pool temperatures for summer 2009/10 (with heating)

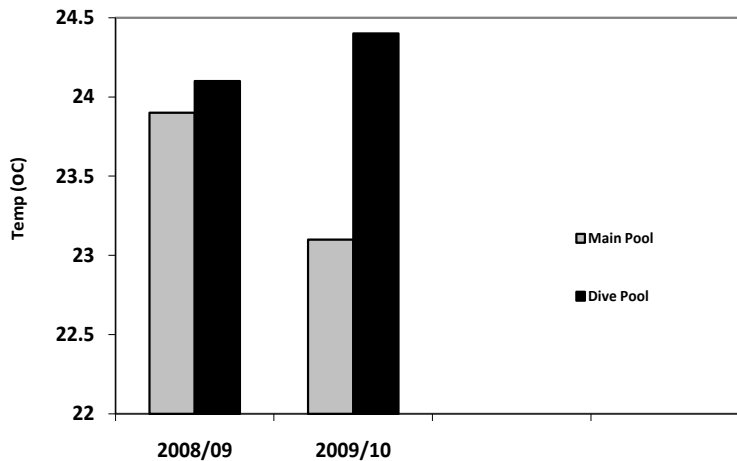


Fig. 10 Average temperature of pools over the 2008/09 (unheated) and 2009/10 (heated) seasons

CONCLUSION AND DISCUSSION

The use of unglazed solar collectors has often been used as a means of providing low cost heating to swimming pools. However, these systems have poor aesthetics due to their lack of integration with the building itself.

This study has examined the development of a novel large area unglazed building integrated solar pool heating system (BIT), based on long run sheet metal roofing, from its initial conceptualisation through to its implementation. In doing this it has demonstrated the process of developing a new solar thermal system from concept to implementation. It also highlights the role that modelling can play in the development of new solar products and discusses the performance of the system in the “as-built” configuration.

Furthermore, it shows that it is possible to integrate solar thermal systems directly into conventional roofing material. Moreover, it shows that this integration can make significant contributions to heating system at the low temperatures found in swimming pools.

REFERENCES

- Anderson, T.N. *et al*, 2007, “A Typical Meteorological Year for Energy Simulations in Hamilton, New Zealand”, *Engineering TreNZ*, 2007-003
- Anderson, T.N. *et al*, 2009, “Performance of a Building Integrated Photovoltaic/Thermal (BIPVT) Solar Collector”, *Solar Energy*, Vol. 83, No. 4, pp. 445-455
- Bartelsen, B. *et al*, 1999, “Elastomer-metal-absorber: development and application”, *Solar Energy*, Vol. 67, Nos. 4–6, pp. 215–226
- Canadian Renewable Energy Network, 2010, *Enerpool Pro*, <http://www.canren.gc.ca>
- Chow, T.T *et al*, 2007, “An experimental study of facade-integrated photovoltaic/water-heating system”, *Applied Thermal Engineering*, Vol. 27, pp. 37–45
- Colon, C.J., and Merrigan, T., 2001, “Roof integrated solar absorbers: The measured performance of “invisible” solar collectors”, *Proceedings of the International Solar Energy Conference 2001*, Washington D.C., pp. 151-159
- Duffie, J.A. and Beckman, W.A., 2006, “*Solar engineering of thermal processes*”, Wiley, New York
- Eicker, U., 2003, *Solar Technologies for Buildings*, John Wiley and Sons, Chichester
- Fuentes, M.K., 1987, “A simplified Thermal Model for Flat-plate Photovoltaic Arrays”, *Sandia National Laboratories Report, SAND85-0330-UC-63*, Albuquerque
- Ji, J. *et al*, 2006, Effect of flow channel dimensions on the performance of a box-frame photovoltaic/thermal collector, *Journal of Power and Energy, Proceedings of the Institution of Mechanical Engineers, Part A*, Vol. 220, No. A7, pp. 681-688
- Kang, M.C. *et al*, 2006, “Numerical analysis on the thermal performance of a roof-integrated flat-plate solar collector assembly”, *International Communications in Heat and Mass Transfer*, Vol. 33, pp. 976–984
- Medved, S. *et al*, 2003, “A large-panel unglazed roof-integrated liquid solar collector—energy and economic evaluation”, *Solar Energy*, Vol. 75, pp. 455–467
- Probst, M.M., and Roecker, C., 2007, “Towards an improved architectural quality of building integrated solar thermal systems (BIST)”, *Solar Energy*, Vol. 81, pp. 1104–1116
- Watmuff, J.H. *et al*, 1977, “Solar and wind induced external coefficients for solar collectors”, *Complex* No. 2 (56).